JPET Fast Forward. Published on January 28, 2005 as DOI: 10.1124/jpet.104.082495

JPET #82495

Angiotensin II Attenuates Synaptic GABA Release and Excites Paraventricular-Rostral Ventrolateral Medulla Output Neurons

De-Pei Li and Hui-Lin Pan

Department of Anesthesiology

Pennsylvania State University College of Medicine

The Milton S. Hershey Medical Center

Hershey, PA 17033

JPET #82495

Running Title: Angiotensin II and Hypothalamic Sympathetic Premotor Neurons

List of abbreviations:

Miniature inhibitory postsynaptic currents (mIPSCs);

Miniature excitatory postsynaptic currents (mEPSCs);

Evoked inhibitory postsynaptic currents (eIPSCs);

Evoked excitatory postsynaptic currents (eEPSCs);

Guanosine 5'-*O*-(2-thiodiphosphate) (GDP-β-S); lidocaine N-ethyl bromide (QX-314)

Intermediolateral cell column (IML); Rostral ventrolateral medulla (RVLM);

Number of text pages: 33

Number of tables: 0; Number of figures: 9

Number of words: Abstract: 248; Introduction: 482; Discussion: 1482;

Number of references: 34

Address for correspondence:

Hui-Lin Pan, M.D., Ph.D.

Department of Anesthesiology, H187

Pennsylvania State University College of Medicine

500 University Drive

Hershey, PA 17033

Tel: (717) 531-8433

Fax: (717) 531-6221

E-mail: hpan@psu.edu

JPET Fast Forward. Published on January 28, 2005 as DOI: 10.1124/jpet.104.082495
This article has not been copyedited and formatted. The final version may differ from this version.

ABSTRACT

The hypothalamic paraventricular nucleus (PVN) neurons regulate sympathetic outflow through projections to the spinal cord and rostral ventrolateral medulla (RVLM). Although the PVN-RVLM pathway is important for the action of brain angiotensin II (Ang II) on autonomic control, the cellular mechanisms involved are not fully known. In this study, we examined the effect of Ang II on the excitability and synaptic inputs to RVLM-projecting PVN neurons. PVN neurons were retrogradely labeled by FluoSpheres injected into the RVLM of rats. Whole-cell patch-clamp recordings were performed on labeled PVN neurons in brain slices. Ang II significantly increased the firing rate of PVN neurons from 3.63 ± 0.65 to 6.10 ± 0.75 Hz ($P < 0.05$, $n = 9$), and such an effect was eliminated by an AT_1 receptor antagonist, losartan. Furthermore, inclusion of a G protein inhibitor, GDP-β-s, in the pipette internal solution did not alter the excitatory effect of Ang II on labeled PVN neurons. Application of 0.5-5 μM Ang II significantly decreased the amplitude of evoked GABAergic IPSCs in a dose-dependent manner. Also, 2 μM Ang II significantly decreased the frequency of mIPSCs from 3.89 ± 0.84 to 2.06 ± 0.45 Hz ($P < 0.05$, $n = 11$) but did not change the amplitude and decay time constant of mIPSCs. By contrast, Ang II had no significant effect on glutamatergic EPSCs at the concentrations that inhibited IPSCs. In addition, Ang II failed to excite PVN neurons in the presence of bicuculline. Collectively, this study provides important new information that Ang II excites RVLM-projecting PVN neurons through attenuation of GABAergic synaptic inputs.

INTRODUCTION

The hypothalamic paraventricular nucleus (PVN) is a heterogenous structure composed of functionally different subsets of neurons and plays an important role in the control of neuroendocrine and autonomic functions (Swanson and Sawchenko, 1983; Dampney, 1994; Allen, 2002). In addition to the projection to sympathetic preganglionic neurons located in the intermediolateral cell column of the spinal cord (IML), the PVN neurons also project to neurons within the rostral ventrolateral medulla (RVLM) (Shafton et al., 1998; Yang and Coote, 1998; Pyner and Coote, 2000; Hardy, 2001). The RVLM is a pivotal structure in maintaining tonic sympathetic nerve activity and basal blood pressure through projections to the IML. The PVN parvocellular neurons project to both the RVLM and IML (Shafton et al., 1998; Pyner and Coote, 2000). Available functional evidence suggests that the PVN-RVLM pathway is important in regulation of sympathetic outflow originated from the PVN (Tagawa and Dampney, 1999; Allen, 2002). In this regard, microinjection of a $GABA_A$ receptor agonist, muscimol, into the PVN decreases the basal blood pressure and sympathetic nerve activity, and this effect is largely eliminated by synaptic blockade of the RVLM in rats (Allen, 2002). However, the cellular mechanisms involved in regulation of the excitability of PVN-RVLM output neurons remain poorly understood.

The renin-angiotensin system plays a critical role in the control of the sympathetic nervous system (Chen and Toney, 2001; Pan, 2004; Wang et al., 2004b). For example, angiotensin II (Ang II) can influence the PVN neurons through activation of receptors in the

circumventricular organs, the regions lacking normal blood-brain barrier (Bains and Ferguson, 1995; Zhang et al., 2002). Also, Ang II may act as a neurotransmitter or modulator in several regions of the hypothalamus including the PVN (Li and Ferguson, 1993; de Wardener, 2001). A major source of the angiotensinergic inputs to PVN neurons is circumventricular organs (Li and Ferguson, 1993; Bains and Ferguson, 1995). Furthermore, the immunoreactivity of angiotensin type 1 (AT_1) receptors and their mRNA are densely distributed in the PVN (Gehlert et al., 1991; Aguilera et al., 1995; Li et al., 2003). The excitability of PVN sympathetic premotor neurons are finely regulated by both inhibitory GABAergic and excitatory glutamatergic synaptic inputs (Li et al., 2002; Li et al., 2003; Li et al., 2004). The excitatory synaptic input to RVLM pressor neurons is important for the action of Ang II in the PVN (Tagawa and Dampney, 1999). We have recently shown that Ang II increases the excitability of spinally projecting PVN neurons by attenuation of GABAergic synaptic inputs (Li et al., 2003). However, the effect of Ang II on the excitability and synaptic inputs to RVLM-projecting PVN neurons is still not clear. Therefore, we determined the effect of Ang II on the excitability and GABAergic and glutamatergic synaptic inputs to RVLM-projecting PVN neurons using a combination of *in vivo* retrograde tracing and *in vitro* whole-cell recordings techniques.

METHODS

Retrograde labeling of RVLM-projecting PVN neurons

Sprague-Dawley rats (200-225 g; Harlan, Indianapolis, IN) of either sex were used for this study. The surgical preparations and experimental protocols were approved by the Animal Care and Use Committee of the Pennsylvania State University College of Medicine and conformed to the NIH guidelines on the ethical use of animals. Rats were anesthetized by i.p. injection of ketamine (70 mg/kg) and xylazine (6 mg/kg) mixture, and the head of the rat was placed in a stereotaxic apparatus. A burr hole (4 mm in diameter) was made in the occipital bone bilaterally according to the following coordinates (bregma): 11.80-13.0 mm caudal, 1.8-2.2 mm lateral, 7.8-8.1 mm deep from the surface of the cortex. A rhodamine-labeled fluorescent microsphere suspension (FluoSpheres, 0.04 μm, Molecular Probes, Eugene, OR) was ejected (Nanojector II, Drummond Scientific Company, Broomall, PA) bilaterally into the region of the RVLM. The pipette was positioned with a micromanipulator and the injection of 50 nl FluoSpheres was monitored through a surgical microscope. After injection, the muscle and skin were sutured and the wound was closed. Animals were returned to their cages for 2-5 days, which is sufficient time to permit retrograde tracer being transported to the PVN.

Slice preparations

Coronal hypothalamic slices (300 μm in thickness) containing the PVN were cut using a vibratome (Technical Product International, St. Louis, MO), as described previously (Li et al.,

2002; Li et al., 2003). Briefly, two to five days after tracer injection, the rats were rapidly decapitated under halothane anesthesia. The brain was quickly removed and placed in ice-cold artificial cerebral spinal fluid (aCSF) perfusion solution saturated with 95% O_2 and 5% CO_2 for 1-2 min. A tissue block containing the hypothalamus was cut from the brain and glued onto the stage of the vibratome. After the sectioning, the slices were pre-incubated in the aCSF, which was continuously gassed with 95% O_2 and 5% CO_2 at 34^{o}C for at least 1 hr until used for recording. For recordings, a slice was transferred to a submersion-type recording chamber, continuously perfused (3 ml/min) with aCSF perfusion solution containing (in mM): 124.0 NaCl, 3.0 KCl, 1.3 $MgSO_4$, 2.4 $CaCl_2$, 1.4 NaH_2PO_4, 10.0 glucose, and 26.0 $NaHCO_3$ saturated with a gas mixture of 95% O_2 and 5% CO_2 at 34^{o}C.

To verify the injection site and diffusion size of FluoSpheres, the brainstem was taken out after sacrificing the rat and immediately sectioned at the injection level. The brainstem slices were viewed and the injection sites of FluoSpheres was identify under a microscope equipped with epifluorescence illumination. The diffusion of the tracer in the RVLM was generally limited to - 11.9 ± 0.05 and -12.4 ± 0.05 mm (bregma), and the diffusion size of FluoSpheres around the site of injection was about 0.4 mm in diameter (Fig. 1A). Rats were excluded if the injection site was not located in the RVLM.

Electrophysiological recordings

Whole-cell voltage- and current-clamp recordings were performed in a radio frequency-shielded room, as we described previously (Li et al., 2002; Li et al., 2003). The recording

pipettes were triple-pulled from borosilicate capillaries (1.2 mm OD, 0.68 mm ID; World Precision Instruments, Sarasota, FL) using a micropipette puller (P-97, Sutter Instrument, Novato, CA). The resistance of the pipette was 3-5 MΩ when it was filled with a solution containing (in mM): 130.0 potassium gluconate, 1.0 $MgCl_2$, 10.0 HEPES, 10.0 EGTA, 1.0 $CaCl_2$, 0.5 Na-GTP, and 4.0 ATP-Mg; adjusted to pH 7.25 with 1 M KOH (290-320 mOsm). The slice was placed in a glass-bottomed recording chamber (Warner Instruments, Hamden, CT) and fixed with a grid of parallel nylon threads supported by a U-shaped stainless steel weight. The slice was perfused at 3.0 ml/min at 34°C maintained by an in-line solution heater and a temperature controller (model TC-324, Warner Instruments). It took about 1.5 min to completely exchange the solution inside the recording chamber at the perfusion speed of 3.0 ml/min. Whole-cell recordings from labeled PVN neurons (Fig. 1 B and C) were made under visual control using a combination of epifluoresence illumination and infrared and differential interference contrast optics on an upright microscope (BX50WI, Olympus, Japan). Because the labeled RVLM-projecting neurons are primarily present in the medial one third of the PVN area between the third ventricle and the fornix, labeled PVN neurons in this site were selected for recording. Recordings were performed using an Axopatch 200B or Multiclamp 700A amplifier (Axon Instruments, Foster City, CA). Signals were filtered at 1-2 kHz, digitized at 10 kHz using Digidata 1320A (Axon Instruments). The series resistance was compensated by 60-80%. The recording was abandoned if the input resistance (measured with a voltage range of 15-20 mV) changed more than 15% during the recording.

Voltage-clamp recordings of postsynaptic currents: Miniature GABAergic inhibitory

postsynaptic currents (mIPSCs) were recorded at a holding potential of 0 mV and in the presence of 1 μM tetrodotoxin (TTX) and 20 μM 6-cyano-7-nitroquinoxaline-2,3-dione (CNQX). The miniature excitatory postsynaptic currents (mEPSCs) were recorded at a holding potential of -70 mV in the presence of 1 μM TTX and 20 μM bicuculline (Li et al., 2002; Li et al., 2003). A general G protein inhibitor, 1 mM guanosine 5'-*O*-(2-thiodiphosphate) (GDP-*β*-*s*, a general G protein inhibitor) was added into the recording pipette solution to block the possible postsynaptic response mediated by G proteins coupled to angiotensin AT_1 receptors (Li et al., 2003). The effective concentration of GDP-β-s to block the postsynaptic effect of Ang II has been shown in previous studies (Ohya and Sperelakis, 1991; Oz and Renaud, 2002). To study the evoked IPSCs and EPSCs (eIPSCs/eEPSCs) in labeled PVN neurons, synaptic currents were evoked by electrical stimulation (0.1 ms, 0.3 - 0.8 mA, and 0.1 Hz) through a bipolar tungsten electrode connected to a stimulator (Grass Instruments, West Warwick, RI). The tip of the stimulating electrode was placed 200 - 600 μm away from the recorded neuron. A Na^+ channel blocker, lidocaine N-ethyl bromide (QX-314, 10 mM) was also included in the pipette solution to block the Na^+ current in these voltage-clamp experiments. Based on the optimal reversal potentials determined for CNQX-sensitive EPSCs and bicuculline-sensitive IPSCs, the eEPSCs and eIPSCs were recorded at a holding potential of -70 and 0 mV, respectively (Li et al., 2003).

To examine the effect of Ang II on the paired-pulse facilitation, two consecutive synaptic responses (A1 and A2) were evoked by a pair of stimulus given at a short interval (40 ms for EPSCs and 50 ms for IPSCs). Paired-pulse facilitation was expressed as the amplitude ratio of the second synaptic response to the first synaptic response (A2/A1).

Current-clamp recordings of firing activity: The spontaneous firing activity of labeled PVN neurons was recorded using the whole-cell current-clamp technique (Li et al., 2003). The recording procedures were similar to those used for postsynaptic current recordings as described above except that TTX and QX-314 were not used. In some experiments, 1 mM GDP-β-s was included in the recording pipette solution to block the postsynaptic effect of Ang II. Recordings of the firing activity of labeled PVN neurons began about 5 min after the whole-cell access was established and the firing activity reached a steady state. Signals were processed, recorded, and analyzed as described above. The junction potential was corrected during off-line analysis.

Drugs were applied to the recording chamber at final concentrations. Ang II, PD123319, CNQX, bicuculline, and *GDP-β-s* were obtained from Sigma (St. Louis, MO). Losartan was a gift from Merck & Co., Inc. (Rahway, NJ). TTX and QX-314 were purchased from Alomone Labs (Jerusalem, Israel). All the drugs were prepared immediately before the experiments and applied to the recording chamber using syringe pumps.

Data analysis

Data are presented as means ± S.E.M. The mIPSCs and mEPSCs were analyzed off-line with a peak detection program (MiniAnalysis, Synaptosoft Inc., Leonia, NJ). Measurements of the averaged firing rate, amplitude, and the decay time constant of postsynaptic currents were performed over a period of 3 min during control, drug application, and recovery. The mIPSCs and mEPSCs were detected by the fast rise time of the signal over an amplitude threshold above the background noise. The amplitude detection threshold was typically 3-5 pA. We manually

excluded the event when the noise was erroneously identified as the mEPSCs or mIPSCs by the program. The background noise level was typically constant throughout the recording of a single neuron. The cumulative probability of the amplitude and interevent interval of mEPSCs/mIPSCs was compared using the Kolmogorov-Smirnov test, which estimates the probability that two cumulative distributions are similar. At least 100 randomly selected mIPSCs and mEPSCs were used in each analysis. All the decay phases of mIPSCs and mEPSCs were analyzed with one and two exponential functions. Based on the curve fitting R^2 values, all mIPSCs were best fitted by two components under all conditions. For cells displaying intermittent firing activity, the membrane potential was measured when the cell was silent and the membrane potential became stable. For those cells showing tonic activity, the membrane potential was usually estimated 200 ms prior to initiation of the action potential (Li et al., 2003). The effects of drugs on the amplitude and frequency of mIPSCs and mEPSCs were determined by the nonparametric Wilcoxon signed rank test or nonparametric ANOVA (Kruskal-Wallis) with Dunn's *post hoc* test. $P < 0.05$ was considered to be statistically significant.

RESULTS

Whole-cell voltage-clamp recordings were obtained from a total of 101 FluoSphere-labeled neurons located in the PVN (n = 47 rats). All recorded neurons displayed membrane potential of -64.3 ± 2.1 mV, input resistance of 489.6 ± 28.3 MΩ, and action potential amplitude of 68.6 ± 3.5 mV.

Effect of Ang II on the firing activity of labeled PVN neurons

To determine the effect of Ang II on the excitability of labeled PVN neurons, the spontaneous firing activity of these neurons were recorded under current-clamp condition. The majority of the labeled PVN neurons tested had spontaneous activity (38 of 48, 79.1%). Ang II, at a concentration of 2 μM, significantly increased the firing rate from 3.63 ± 0.65 to 6.10 ± 0.75 Hz in all 9 cells tested (Fig. 2). However, the membrane potential was not significantly altered by 2 μM Ang II (-64.8 ± 2.01 to -63.5 ± 2.2 mV; $P > 0.05$; n = 9). Repeat applications of 2 μM Ang II produced a similar increase in firing rate in these labeled PVN neurons (Fig. 2 A and B). To examine if the excitatory effect of Ang II was mediated through postsynaptic angiotensin receptors, 1 mM GDP-β-s was included in the pipette internal solution to block the possible postsynaptic effect of Ang II in additional 8 labeled PVN neurons. There was no significant alteration of the membrane potential and firing activity during the course of intracellular dialysis of GDP-β-s (the first 3-5 min after rupturing the cell membrane). Perfusion of 2 μM Ang II still increased the firing rate of these labeled PVN neurons from 1.99 ± 0.33 to

4.6 ± 0.63 Hz ($P < 0.05$; Fig. 2C). There was no significant difference between the excitatory effect of Ang II on the firing rate of cells recorded with and without GDP-β-s inside the electrode.

To further determine the receptor subtype that mediated the effect of Ang II on the firing activity of the PVN neurons, the specific antagonists for the AT_1 (losartan) and AT_2 (PD 123319) receptors were used. The effective concentrations of these antagonists have been determined previously (Li et al., 2003). Ang II (2 μM) failed to increase the firing rate of 9 labeled PVN neurons in the presence of 2 μM losartan (4.32 ± 0.91 vs. 4.44 ± 0.88 Hz, $P > 0.05$, Fig. 3A and B). However, 5 μM PD 123319 did not affect the excitatory effect of 2 μM Ang II on another 7 labeled PVN neurons. Ang II increased the firing rate from 3.13 ± 0.76 to 5.50 ± 1.08 Hz ($P < 0.05$) in these 7 cells in the presence of PD123319 (Fig. 3C).

Effect of Ang II on eIPSCs and eEPSCs of labeled PVN neurons

Because inclusion of GDP-β-s in the pipette solution did not affect the excitatory effect of Ang II on labeled PVN cells, we next determined the possible effect of Ang II on the synaptic inputs to the PVN neurons. Both IPSCs and EPSCs were evoked by electrical stimulation at a constant intensity. The eEPSCs were recorded at a holding potential of -70 mV, while the eIPSCs was isolated at a holding potential of 0 mV (Li et al., 2003). The eIPSCs were completely eliminated by application of 20 μM bicuculline and the eEPSCs were abolished by application of 20 μM CNQX (Fig. 4A). Both eEPSCs and eIPSCs were evoked in 10 of 14 labeled PVN neurons, and only eIPSCs were elicited without detectable eEPSCs in the

remaining 4 cells. Ang II (0.5-5 μM) inhibited the peak amplitude of eIPSCs in a concentration-dependent manner (n = 14, Fig. 4A). The peak amplitude of eIPSCs was reduced by Ang II at a concentration of 0.5 μM and the inhibition reached the maximum (~52.7%) at a concentration of 2 μM (Fig. 4B). In contrast, Ang II had little effect on the amplitude of eEPSCs even at a higher concentration (5 μM, n = 10, Fig. 4). Furthermore, Ang II did not significantly alter the holding current and input resistance in these 14 labeled PVN neurons. The holding current was 78.2 ± 8.5 and 76.1 ± 8.9 pA during control and application of 2 μM Ang II, respectively, at a holding potential of 0 mV. When the cell was voltage-clamped at -70 mV, the holding current was -19.6 ± 3.5 and -20.6 ± 3.8 pA before and during application of 2 μM Ang II, respectively. The input resistence before and during perfusion of 2 μM Ang II was 481.1 ± 23.6 and 473.6 ± 35.9 MΩ, respectively ($P > 0.05$; n = 14).

Effect of Ang II on mIPSCs and mEPSCs of labeled PVN neurons

To further determine the presynaptic effect of Ang II in labeled PVN neurons, we tested the effect of 2 μM Ang II on the mIPSCs and mEPSCs. The mIPSCs were recorded in the presence of 1 μM TTX and 20 μM CNQX. The mIPSCs were completely abolished by 20 μM bicuculline (Fig. 5A). Ang II significantly decreased the frequency of mIPSCs from 3.89 ± 0.84 to 2.06 ± 0.45 Hz ($P < 0.05$; n = 11) without affecting the amplitude and decay time constant of mIPSCs in a concentration of 2 μM (Fig. 5). The cumulative probability analysis of mIPSCs before and during Ang II application revealed that the distribution pattern of the interevent interval of mIPSCs shifted to the right in response to Ang II, whereas the distribution pattern of

the amplitude of mIPSCs was not changed (Fig. 5B and C). The decay phase of mIPSCs was best fitted by a double-exponential function (Fig. 5D). Neither the fast (6.87 ± 0.38 vs. 6.89 ± 0.47 ms) nor slow (21.91 ± 1.28 vs. 22.32 ± 2.35 ms) components of the decay phase of mIPSCs during Ang II application was significantly different from those during the control. Repeat application of Ang II had a reproducible inhibitory effect on the frequency of mIPSCs in these 11 labeled PVN neurons (data not shown).

The effect of Ang II on mEPSCs was tested in another 9 labeled PVN neurons. The mEPSCs were recorded at a holding potential of -70 mV in the presence of 1 μM TTX and 20 μM bicuculline. In these 9 neurons tested, the mEPSCs were completely abolished by 20 μM CNQX (Fig. 6A). Neither the frequency nor the amplitude of mEPSCs was significantly affected by bath application of 2 and 5 μM Ang II (Fig. 6). The effect of Ang II on mEPSCs was further analyzed by measuring the time constant of the decay phase of mEPSCs. The decay phase of mEPSCs was best fitted by a single-exponential function (Fig. 6D). The decay time constants of mEPSCs were similar during control and Ang II application (2.58 ± 0.96 vs. 2.46 ± 0.81 ms; $P > 0.05$; n = 9).

To define the receptor subtype mediating the effect of Ang II on mIPSCs, losartan and PD123319 were used. In all 11 labeled PVN neurons, 2 μM losartan completely blocked the inhibitory effect of 2 μM Ang II on the frequency of mIPSCs (Fig. 7). Losartan alone had no effect on mIPSCs of these neurons in the slice preparation. The frequency (2.43 ± 0.55 vs. 2.40 ± 0.52 Hz, $P > 0.05$) and amplitude (40.53 ± 3.6 vs. 39.6 ± 3.4 pA, $P > 0.05$) of mIPSCs were not significantly altered by bath application of Ang II in the presence of losartan. However, 2

μM Ang II still significantly decreased the frequency of mIPSCs from 2.35 ± 0.67 to 1.09 ± 0.26 ($P < 0.05$) in the presence of 5 μM PD123319 in 8 separated labeled PVN neurons tested (Fig. 7 F and G).

Effect of Ang II on paired-pulse facilitation of evoked IPSCs and EPSCs

To further determine the presynaptic effect of Ang II, we examined the effect of 2 μM Ang II on paired-pulse ratio (PPR) of evoked IPSCs and EPSCs in 9 separate labeled PVN neurons. Ang II increased the PPR (A2/A1) of evoked IPSCs from 1.22 ± 0.06 to 1.56 ± 0.07 in 8 of 9 labeled PVN neurons ($P < 0.05$, Fig. 8 A and B). Ang II did not change the PPR of evoked IPSCs in the remaining 1 neuron (1.02 vs 1.03). On the other hand, 2 μM Ang II did not significantly change the PPR of evoked EPSCs in all 6 labeled PVN neurons tested (Fig. 8C).

Effect of Ang II and bicuculline on the firing activity of labeled PVN neurons

Because Ang II selectively reduced inhibitory GABAergic inputs to labeled PVN cells, we subsequently determined if Ang II-induced disinhibition was responsible for the excitatory effect of Ang II on PVN-RVLM neurons. Thus, the effect of 2 μM Ang II on the firing activity of labeled PVN neurons was tested in the presence of the $GABA_A$ receptor antagonist bicuculline. The spontaneous activity of 8 labeled PVN neurons was significantly increased by initial application of 2 μM Ang II and following application of 20 μM bicuculline (Fig. 9A). Bicuculline along significantly increased the firing rate from 2.86 ± 0.54 to 5.54 ± 0.69 Hz and depolarized the cell membrane from -64.8 ± 1.6 to -60.9 ± 2.0 mV (n = 8, $P < 0.05$). However,

JPET Fast Forward. Published on January 28, 2005 as DOI: 10.1124/jpet.104.082495
This article has not been copyedited and formatted. The final version may differ from this version.

subsequent application of 2 μM Ang II failed to further increase the firing rate of these neurons in the presence of 20 μM bicuculline (Fig. 9 A and B). Lack of effect of Ang II in the presence of bicuculline could be possibly due to that bicuculline had maximally increased the firing activity of these neurons. To examine this possibility, capsaicin was further applied in the presence of bicuculline. Capsaicin in a concentration of 1 μM (Li et al., 2004) still significantly increased the firing activity from 4.72 ± 0.42 to 6.09 ± 0.48 Hz (Fig. 9 C and D; $P < 0.05$; n = 7) in the presence of 20 μM bicuculline (Fig. 9 C and D).

DISCUSSION

The hypothalamic PVN is a heterogenous structure that contains magnocellular neuroendocrine neurons as well as parvocellular sympathetic premotor neurons (Swanson and Sawchenko, 1983; Ranson et al., 1998; Yang and Coote, 1998; Pyner and Coote, 2000; Hardy, 2001). Although the PVN sympathetic premotor neurons send projections to both the RVLM and IML, the relative functional importance of these two pathways in autonomic regulation remains to be established. Our previous studies have focused largely on cellular mechanisms involved in the control of PVN-IML projection neurons (Li et al., 2002; Li et al., 2003). It has been shown that inhibition of the PVN decreases the basal blood pressure and sympathetic nerve activity, an effect that is largely attenuated by synaptic blockade of the RVLM in rats (Allen, 2002). Thus, the PVN-RVLM pathway appears to be more important for regulation of sympathetic outflow and blood pressure. In this electrophysiological study, we used a combination of retrograde labeling and *in vitro* brain slice whole-cell recording techniques to specifically determined the cellular mechanisms responsible for the excitatory effect of Ang II on RVLM-projecting PVN neurons.

Both anatomical and functional evidence suggest that the PVN plays an important role in the regulation of autonomic function by Ang II (Pan, 2004). For instance, the sympathoexcitatory response induced by central hyperosmolality is attenuated by blockade of AT_1 receptors with losartan in the PVN (Chen and Toney, 2001). We found that Ang II significantly increased the firing rate of labeled PVN neurons, and such an effect was eliminated

by an AT_1 antagonist, losartan, but not by the AT_2 antagonist PD 123319 (Li et al., 2003). Thus, the effect of Ang II on RVLM-projecting PVN neurons is mediated by AT_1, but not AT_2, receptors. These data are consistent with previous studies showing the presence of AT_1 receptors and their mRNA in the PVN (Gehlert et al., 1991; Obermuller et al., 1991; Aguilera et al., 1995; Li et al., 2003). Although the AT_2 receptor immunoreactivity in the PVN has been reported, there is no binding site for AT_2 receptors in the PVN (Gehlert et al., 1991; Song et al., 1992). It is known that the AT1 receptors are G protein-coupled receptors (Richards et al., 1999; Pan, 2004). Surprisingly, however, in the present study the effect Ang II on the firing activity was not affected by inclusion of a general G protein inhibitor, GDP-β-s, in the recording pipette solution. Although Ang II induces a small membrane depolarization in the PVN magnocellular neurons by inhibition of a potassium current (Li and Ferguson, 1996), we observed that Ang II had no detectable postsynaptic effect on the RVLM-projecting PVN neurons in this slice preparation. Notably, it has been reported that puff application of Ang II produces an inward current in some RVLM-projecting PVN neurons (Cato and Toney, 2004), although the pre- and postsynaptic effects of Ang II are not differentiated in that study. The absence of postsynaptic action of Ang II cannot be explained by the dose used in this study. We observed that the excitatory effect of 2 μM Ang II on the firing activity was not affected by intracellular application of GDP-β-s. This suggests that postsynaptic AT_1 receptors do not contribute significantly to the excitatory effect of Ang II on the firing activity of RVLM-projecting PVN neurons.

We thus further examined the possible synaptic mechanisms involved in the effect of

Ang II on RVLM-projecting PVN neurons. We found that Ang II significantly inhibited the evoked GABAergic IPSCs in a concentration-dependent manner. Furthermore, Ang II increased the paired pulse ratio of evoked IPSCs and decreased the frequency of GABAergic mIPSCs without affecting the amplitude and decay time constant of mIPSCs, suggesting that the likely site of its action is at the presynaptic GABAergic terminal. The effect of Ang II on mIPSCs of RVLM-projecting PVN neurons was completely blocked by a selective AT_1 receptor antagonist, losartan. But the specific AT_2 receptor antagonist PD123319 did not alter the effect of Ang II on mIPSCs and the firing activity of the RVLM-projecting PVN neurons. This finding is consistent with our recent study showing that the AT_1 receptors are located at the presynaptic terminals in the PVN (Li et al., 2003). In contrast to its action on GABAergic IPSCs, Ang II had no significant effect on glutamatergic evoked EPSCs or mEPSCs of labeled PVN neurons at concentrations that attenuated GABAergic IPSCs. The reason for this selective effect of Ang II on the GABAergic synaptic inputs remains unclear. Both nitric oxide and Ang II also preferentially alter GABAergic, but not glutamatergic, synaptic inputs to spinally projecting PVN neurons (Li et al., 2002; Li et al., 2003). On the other hand, the vanilloid receptor-1 (TRPV1) agonist capsaicin selectively enhances the glutamatergic, but not GABAergic, synaptic inputs to these PVN neurons (Li et al., 2004). Because Ang II only inhibits GABAergic synaptic inputs to the labeled PVN neurons, it is possible that the glutamatergic terminals which make synapse with PVN-RVLM output neurons have no sufficient functional AT_1 receptors. The signal transduction mechanisms underlying the effect of Ang II on the synaptic GABA release remain largely unidentified. Ang II receptors are coupled to different types of G-proteins

resulting in activation of many different signaling pathways including phospholipase C, D and A2, protein kinase C, and delayed rectifier and transient A-type K^+ currents (Dudley et al., 1990; Pueyo et al., 1996; Sumners et al., 1996; Richards et al., 1999). Recent studies also suggest that the reactive oxygen species may be involved in the action of Ang II in the brain (Zimmerman et al., 2002; Wang et al., 2004a). Further studies are warranted to define the signaling mechanisms of the presynaptic effect of Ang II in the PVN.

To determine if attenuation of GABAergic synaptic inputs contributes to Ang II-induced excitation of these PVN neurons, we determined the effect of Ang II on the firing activity of labeled PVN neurons following blockade of $GABA_A$ receptors with bicuculline. We found that Ang II failed to excite the labeled PVN neurons in the presence of bicuculline, suggesting that the excitatory effect of Ang II on RVLM-projecting PVN neurons is mediated by a disinhibition (reduction of GABAergic inputs) mechanism. Bicuculline alone produced a profound increase in the firing activity in all labeled PVN neurons tested. Hence, these PVN output neurons are under a tonic inhibition by the GABAergic synaptic inputs, and GABA acts as a shunt to maintain a hyperpolarized membrane potential and restrain firing. This tonic GABAergic inhibition of PVN output neurons appears to be similar to modulation of the background firing of thalamocortical neurons by inhibitory sculpturing (Steriade et al., 1993). It is possible that lack of effect of Ang II on the firing activity in the presence of bicuculline may be due to the maximal firing of PVN neurons following bicuculline. Capsaicin excites PVN pre-autonomic neurons through selective potentiation of glutamatergic inputs (Li et al., 2004). Thus, we applied capsaicin in the presence of bicuculline to examine this possibility. We found that

capsaicin still caused a significant increase in the firing activity of labeled PVN neurons in the presence of bicuculline. Therefore, these data provide strong evidence that attenuation of GABAergic synaptic inputs is ultimately involved in the excitatory effect of Ang II on RVLM-projecting PVN neurons. Ang II could excite PVN sympathetic premotor neurons to augment sympathetic outflow by attenuation of synaptic GABA release.

Although PVN neurons project to both the IML and RVLM (Shafton et al., 1998; Pyner and Coote, 2000), there are some major differences as to the proportions of PVN neurons projecting to either the RVLM or IML. When the retrograde tracer is injected into the caudal spinal cord at T13-L1, about one-third of retrogradely labeled PVN neurons project to both the spinal cord and RVLM (Shafton et al., 1998). However, only about 3% PVN neurons have projections both to the RVLM and IML if the tracer is injected into the rostral spinal cord at T2-T4 level (Pyner and Coote, 2000). Notably, we injected the tracer into the T2-T4 level of the spinal cord in the previous study (Li et al., 2003). Based on that, it is likely that at least large part of the neurons sampled in the present study are different from those studied previously (Li et al., 2003). In general, we found that Ang II has a similar effect on the excitability and GABAergic and glutamatergic synaptic inputs to the two populations of neurons with projections to the spinal cord and RVLM (Li et al., 2003). For example, Ang II increased the firing rate of spinally projecting PVN neurons and RVLM-projecting PVN neurons by 89.2% and 86.6%, respectively. Also, Ang II caused a comparable reduction in the frequency of mIPSCs in spinally projecting PVN neurons and RVLM-projecting PVN neurons (54.5% and 49.8%, respectively). Furthermore, Ang II, in a similar concentration range, decreased the

amplitude of eIPSCs in both spinally projecting and RVLM-projecting PVN neurons. Therefore, the present study, together with our recent finding, provides important information that Ang II has a very similar presynaptic effect on these two populations of PVN sympathetic premotor neurons.

In summary, this study provides new information about the synaptic mechanisms underlying the stimulatory effect of Ang II on RVLM-projecting PVN neurons. This information is important for our understanding of the cellular mechanisms of Ang II in regulation of sympathetic outflow in the hypothalamus. The intrinsic brain Ang II or circulating Ang II could influence the sympathetic outflow through its presynaptic effect on sympathetic premotor neurons in the PVN. Thus, Ang II can regulate sympathetic output and hemodynamics through the PVN-IML, PVN-RVLM, or both pathways. The potential functional difference and differential roles of these two descending projections in the regulation of sympathetic drive under physiological and pathophysiological conditions are currently unclear and should be further investigated.

REFERENCES

Aguilera G, Kiss A and Luo X (1995) Increased expression of type 1 angiotensin II receptors in the hypothalamic paraventricular nucleus following stress and glucocorticoid administration. *J Neuroendocrinol* **7**:775-783.

Allen AM (2002) Inhibition of the hypothalamic paraventricular nucleus in spontaneously hypertensive rats dramatically reduces sympathetic vasomotor tone. *Hypertension* **39**:275-280.

Bains JS and Ferguson AV (1995) Paraventricular nucleus neurons projecting to the spinal cord receive excitatory input from the subfornical organ. *Am J Physiol* **268**:R625-633.

Cato MJ and Toney GM (2004) Angiotensin II excites paraventricular nucleus neurons that innervate the rostral ventrolateral medulla: an in vitro patch-clamp study in brain slices. *J Neurophysiol*: in press.

Chen QH and Toney GM (2001) AT(1)-receptor blockade in the hypothalamic PVN reduces central hyperosmolality-induced renal sympathoexcitation. *Am J Physiol Regul Integr Comp Physiol* **281**:R1844-1853.

Dampney RA (1994) Functional organization of central pathways regulating the cardiovascular system. *Physiol Rev* **74**:323-364.

de Wardener HE (2001) The hypothalamus and hypertension. *Physiol Rev* **81**:1599-1658.

Dudley DT, Panek RL, Major TC, Lu GH, Bruns RF, Klinkefus BA, Hodges JC and Weishaar RE (1990) Subclasses of angiotensin II binding sites and their functional significance.

Mol Pharmacol **38**:370-377.

Gehlert DR, Gackenheimer SL and Schober DA (1991) Autoradiographic localization of subtypes of angiotensin II antagonist binding in the rat brain. *Neuroscience* **44**:501-514.

Hardy SG (2001) Hypothalamic projections to cardiovascular centers of the medulla. *Brain Res* **894**:233-240.

Li DP, Chen SR and Pan HL (2002) Nitric oxide inhibits spinally projecting paraventricular neurons through potentiation of presynaptic GABA release. *J Neurophysiol* **88**:2664-2674.

Li DP, Chen SR and Pan HL (2003) Angiotensin II stimulates spinally projecting paraventricular neurons through presynaptic disinhibition. *J Neurosci* **23**:5041-5049.

Li DP, Chen SR and Pan HL (2004) VR1 receptor activation induces glutamate release and postsynaptic firing in the paraventricular nucleus. *J Neurophysiol* **92**:1807-1816.

Li Z and Ferguson AV (1993) Subfornical organ efferents to paraventricular nucleus utilize angiotensin as a neurotransmitter. *Am J Physiol* **265**:R302-309.

Li Z and Ferguson AV (1996) Electrophysiological properties of paraventricular magnocellular neurons in rat brain slices: modulation of IA by angiotensin II. *Neuroscience* **71**:133-145.

Obermuller N, Unger T, Culman J, Gohlke P, de Gasparo M and Bottari SP (1991) Distribution of angiotensin II receptor subtypes in rat brain nuclei. *Neurosci Lett* **132**:11-15.

Ohya Y and Sperelakis N (1991) Involvement of a GTP-binding protein in stimulating action of angiotensin II on calcium channels in vascular smooth muscle cells. *Circ Res* **68**:763-

771.

Oz M and Renaud LP (2002) Angiotensin AT(1)-receptors depolarize neonatal spinal motoneurons and other ventral horn neurons via two different conductances. *J Neurophysiol* **88**:2857-2863.

Pan HL (2004) Brain angiotensin II and synaptic transmission. *Neuroscientist* **10**:422-431.

Pueyo ME, N'Diaye N and Michel JB (1996) Angiotensin II-elicited signal transduction via AT1 receptors in endothelial cells. *Br J Pharmacol* **118**:79-84.

Pyner S and Coote JH (2000) Identification of branching paraventricular neurons of the hypothalamus that project to the rostroventrolateral medulla and spinal cord. *Neuroscience* **100**:549-556.

Ranson RN, Motawei K, Pyner S and Coote JH (1998) The paraventricular nucleus of the hypothalamus sends efferents to the spinal cord of the rat that closely appose sympathetic preganglionic neurones projecting to the stellate ganglion. *Exp Brain Res* **120**:164-172.

Richards EM, Raizada MK, Gelband CH and Sumners C (1999) Angiotensin II type 1 receptor-modulated signaling pathways in neurons. *Mol Neurobiol* **19**:25-41.

Shafton AD, Ryan A and Badoer E (1998) Neurons in the hypothalamic paraventricular nucleus send collaterals to the spinal cord and to the rostral ventrolateral medulla in the rat. *Brain Res* **801**:239-243.

Song K, Allen AM, Paxinos G and Mendelsohn FA (1992) Mapping of angiotensin II receptor subtype heterogeneity in rat brain. *J Comp Neurol* **316**:467-484.

Steriade M, Contreras D, Curro Dossi R and Nunez A (1993) The slow (< 1 Hz) oscillation in

reticular thalamic and thalamocortical neurons: scenario of sleep rhythm generation in interacting thalamic and neocortical networks. *J Neurosci* **13**:3284-3299.

Sumners C, Zhu M, Gelband CH and Posner P (1996) Angiotensin II type 1 receptor modulation of neuronal K+ and Ca2+ currents: intracellular mechanisms. *Am J Physiol* **271**:C154-163.

Swanson LW and Sawchenko PE (1983) Hypothalamic integration: organization of the paraventricular and supraoptic nuclei. *Annu Rev Neurosci* **6**:269-324.

Tagawa T and Dampney RA (1999) AT(1) receptors mediate excitatory inputs to rostral ventrolateral medulla pressor neurons from hypothalamus. *Hypertension* **34**:1301-1307.

Wang G, Anrather J, Huang J, Speth RC, Pickel VM and Iadecola C (2004a) NADPH oxidase contributes to angiotensin II signaling in the nucleus tractus solitarius. *J Neurosci* **24**:5516-5524.

Wang H, Huang BS, Ganten D and Leenen FH (2004b) Prevention of sympathetic and cardiac dysfunction after myocardial infarction in transgenic rats deficient in brain angiotensinogen. *Circ Res* **94**:843.

Yang Z and Coote JH (1998) Influence of the hypothalamic paraventricular nucleus on cardiovascular neurones in the rostral ventrolateral medulla. *J Physiol* **513**:521-530.

Zhang ZH, Francis J, Weiss RM and Felder RB (2002) The renin-angiotensin-aldosterone system excites hypothalamic paraventricular nucleus neurons in heart failure. *Am J Physiol Heart Circ Physiol* **283**:H423-433.

Zimmerman MC, Lazartigues E, Lang JA, Sinnayah P, Ahmad IM, Spitz DR and Davisson RL

(2002) Superoxide mediates the actions of angiotensin II in the central nervous system. *Circ Res* **91**:1038-1045.

Footnotes

This study was supported by grants from the National Institutes of Health (HL60026 and HL77400) and a Beginning Grant-in-Aid from the American Heart Association, Pennsylvania-Delaware Affiliate. We thank C. Yang for her technical assistance.

Figure Legends

Figure 1. Identification of retrogradely labeled RVLM-projecting PVN neurons

A: Photomicrograph depicting the FluoSphere injection site (red) at the level of the RVLM (Bregma -12.30 mm) in one rat. B: A FluoSphere-labeled PVN neuron in the slice viewed with fluorescence illumination. C: Photomicrograph of the same neuron (*) shown in B with an attached recording electrode (^) in the slice viewed with differential interference contrast optics. Scale bars are 1 mm in A and 50 μm in B and C.

Figure 2. Excitatory effect of Ang II on the firing activity of labeled PVN neurons

A: Upper panel: Histogram showing the reproducible effect of 2 μM Ang II on the firing activity of a labeled PVN neuron. Lower panel: Raw tracings showing the spontaneous discharge activity of the same cell during control, application of 2 μM Ang II, and washout. B and C: Summary data showing the effect of Ang II on the firing activity of labeled PVN neurons recorded using pipette internal solution with (C, n = 8) and without (B, n = 9) 1 mM GDP-β-s. Data presented as means ± S.E.M. * $P < 0.05$ compared to the control (Kruskal-Wallis ANOVA followed by Dunn's post hoc test). Ang II: angiotensin II.

Figure 3. Effect of losartan and PD123319 on Ang II-induced excitation of labeled PVN neurons

A: Upper panel: Histogram showing the effect of losartan on the Ang II-induced excitation of a

PVN neuron. Lower panel: Raw tracings showing the firing activity of the same cell during control, application of 2 μM Ang II, and 2 μM Ang II plus 2 μM losartan. B: Summary data showing the blocking effect of losartan on the Ang II-induced increase in firing activity of 9 labeled PVN neurons. C: Summary data showing lack of blocking effect on 5 μM PD123319 on the excitatory effect of 2 μM Ang II on 7 labeled PVN neurons. Data presented as means ± S.E.M. * $P < 0.05$ compared to the control (Kruskal-Wallis ANOVA followed by Dunn's post hoc test). Ang II: angiotensin II; LST: losartan.

Figure 4. Effect of Ang II on evoked IPSCs and EPSCs in labeled PVN neurons

A: Upper panel: Original recordings showing that Ang II concentration-dependently decreased eIPSCs. The eIPSCs were elicited at a holding potential of 0 mV. Lower panel: Ang II had no effect on eEPSCs recorded at a holding potential of -70 mV. The stimulation artifacts are removed for clarity and indicated by arrows. B: Summary data showing differential effect of 0.5 - 5.0 μM Ang II on eIPSCs (n = 14) and eEPSCs (n = 10). Data presented as means ± S.E.M. * $P < 0.05$ compared to control (Kruskal-Wallis ANOVA followed by Dunn's post hoc test). Ang II: angiotensin II. HP: holding potential.

Figure 5. Effect of Ang II on mIPSCs in labeled PVN neurons

A: Representative tracings from a labeled PVN neuron showing mIPSCs recorded during control, application of 2 μM Ang II, washout, and application of 20 μM bicuculline. B and C: Cumulative probability plot analysis of mIPSCs of the same neuron showing the distributions of

the inter-event interval (B) and peak amplitude (C) during control, Ang II application, and washout. Ang II increased the inter-event interval of mIPSCs ($P < 0.05$, Kolmgorov-Smirnov test) without changing the distribution of the amplitude. (D): Superimposed averages of 100 consecutive mIPSCs obtained during control and Ang II application. The decay phase of mIPSCs was best fitted with a double exponential function. Both τ_{fast} (6.63 vs. 6.71 ms) and τ_{slow} (19.35 vs. 19.69 ms) of the decay phase during control and Ang II administration were similar. E and F: Summary data showing the effect of 2 μM Ang II on the frequency (E) and amplitude (F) of mIPSCs in 11 labeled PVN neurons. Data presented as means ± S.E.M. * $P <$ 0.05 compared to the control (Kruskal-Wallis ANOVA followed by Dunn's post hoc test). Ang II: angiotensin II.

Figure 6. Lack of effect of Ang II on mEPSCs in labeled PVN neurons

A: Representative tracings from a labeled PVN neuron showing mEPSCs during control and application of 5 μM Ang II. B and C: Cumulative plot analysis of mEPSCs of the same neuron showing the distributions of the inter-event interval (B) and amplitude (C) during control and application of 5 μM Ang II. D: Superimposed averages of 100 consecutive mEPSCs obtained during control and Ang II application. The decay phase of mEPSCs was best fitted with a single exponential function. The decay time constant was similar during control (τ=2.42 ms) and Ang II application (τ=2.39 ms). E and F: Summary data showing the effect of 5 μM Ang II on the frequency (E) and amplitude (F) of mEPSCs in 9 labeled PVN neurons. Data presented as means ± S.E.M. Ang II: angiotensin II.

Figure 7. Effect of losartan and PD123319 on Ang II-induced decrease in mIPSCs

A: Raw tracings from a labeled PVN neuron showing mIPSCs recorded during control, application of 2 μM Ang II, and 2 μM losartan plus Ang II. B and C: Cumulative probability plot analysis of mIPSCs of the same neuron showing the distributions of the inter-event interval (B) and peak amplitude (C) during control, Ang II application, and losartan plus Ang II. D and E: Summary data showing the blocking effect of losartan on Ang II-induced inhibition of mIPSCs in 11 labeled PVN neurons. F and G: Summary data showing lack of effect of 5 μM PD123319 on Ang II-induced decrease in mIPSCs of another 8 labeled PVN neurons. Data presented as means ± S.E.M. * $P < 0.05$ compared to the control (Kruskal-Wallis ANOVA followed by Dunn's post hoc test). Ang II: angiotensin II. LST: losartan.

Figure 8. Effect of Ang II on the paired-pulse ratio (PPR) of evoked IPSCs and EPSCs

A, Raw tracings from a labeled PVN neurons showing IPSCs evoked by a paired-pulse stimulation during control and application 2 μM Ang II. The paired-pulse interval was 50 ms. The traces are averages of 10 consecutive responses. The stimulation artifacts are removed for clarity and indicated by arrows. The current recorded during Ang II application was normalized to the first IPSC obtained during control, which shows that PPR was increased by Ang II. B, C, Summary data showing the effect of Ang II on the PPR of evoked IPSCs (B, n = 8) and evoked EPSCs (C, n = 6) in labeled PVN neurons. Data are presented as means ± SEM. * $P < 0.05$, compared with the control (Wilcoxon rank test). Ang II: angiotensin II.

Figure 9. Effects of Ang II and capsaicin on the firing activity of labeled PVN neurons in the presence of bicuculline

A: Upper panel: Histogram showing the effect of 2 μM Ang II, 20 μM bicuculline, and 2 μM Ang II plus 20 μM bicuculline on the firing activity of a labeled PVN neuron. Lower panel: Original tracings recorded during control, application of 2 μM Ang II, 20 μM bicuculline, and Ang II plus bicuculline. B: Summary data showing the effect of 2 μM Ang II on the firing activity of 8 labeled PVN neurons before and after application of 20 μM bicuculline. C: Upper panel: Histogram showing the effect of 2 μM Ang II, 20 μM bicuculline, and 1 μM capsaicin plus 20 μM bicuculline on the firing activity of a labeled PVN neuron. Lower panel: Original tracings recorded during control, Ang II, bicuculline, and capsaicin plus bicuculline. Note that capsaicin further increased the firing activity in the presence of bicuculline. D: Summary data showing the effect of 2 μM Ang II, 20 μM bicuculline, and 1 μM capsaicin plus 20 μM bicuculline on the firing activity of 7 labeled PVN neurons. Data presented as means ± S.E.M. * $P < 0.05$ compared to the control; # $P < 0.05$ compared to the bicuculline alone (Kruskal-Wallis ANOVA followed by Dunn's post hoc test). Ang II: angiotensin II; Bic: bicuculline; Caps: capsaicin.

JPET Fast Forward. Published on January 28, 2005 as DOI: 10.1124/jpet.104.082495
This article has not been copyedited and formatted. The final version may differ from this version.

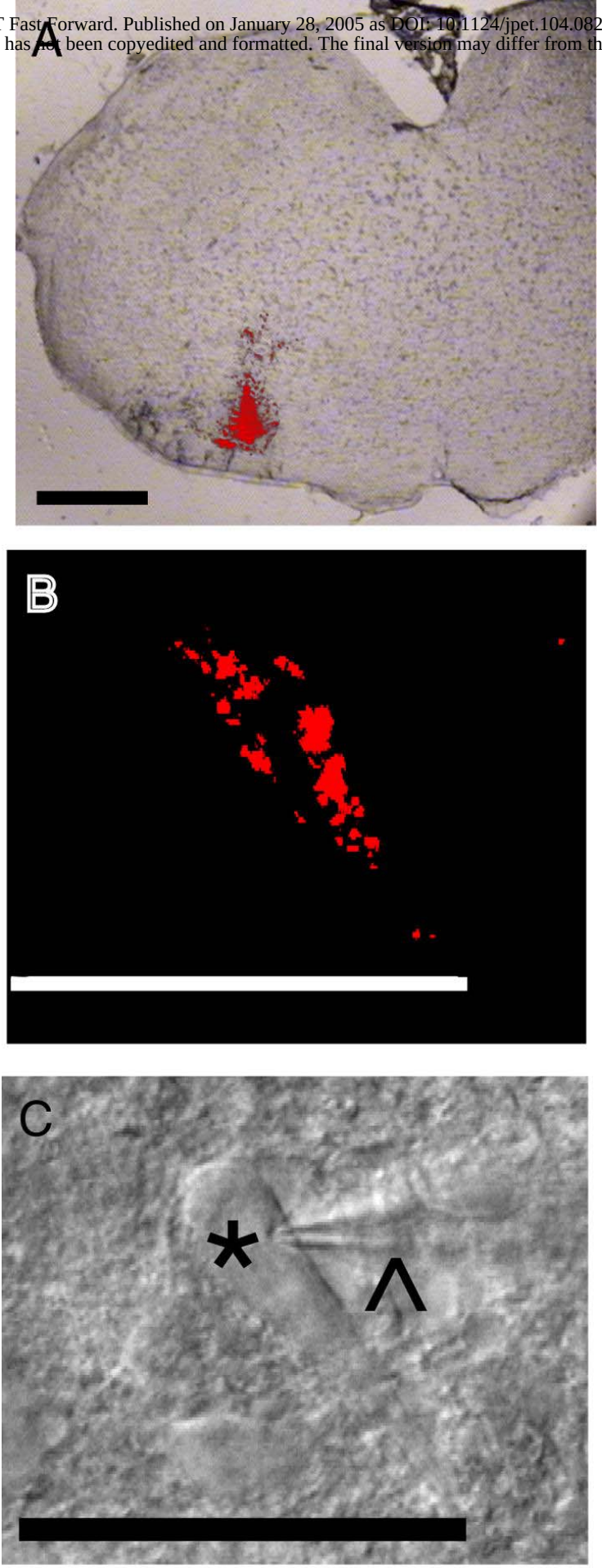

Fig. 1

JPET Fast Forward. Published on January 28, 2005 as DOI: 10.1124/jpet.104.082495
This article has not been copyedited and formatted. The final version may differ from this version.

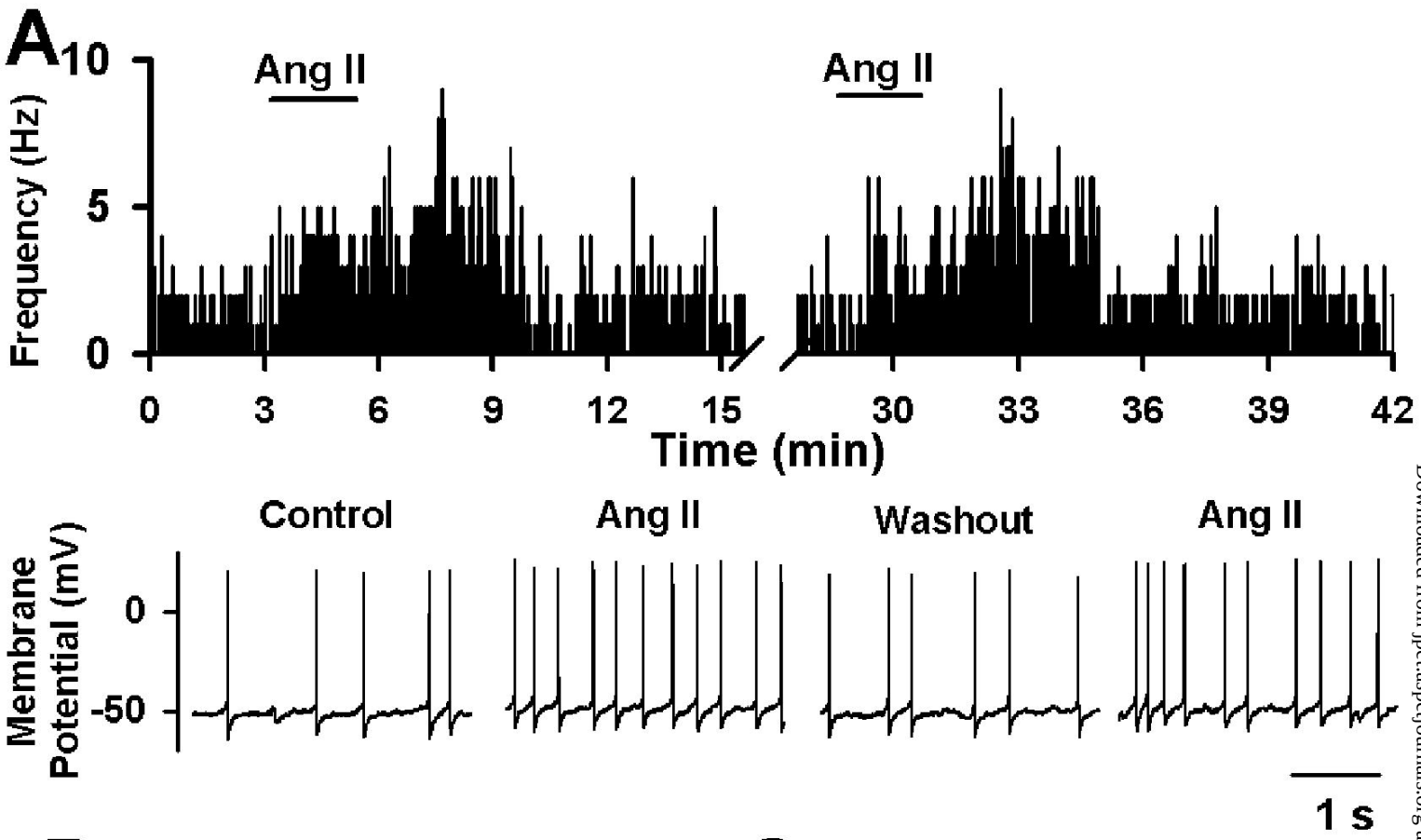

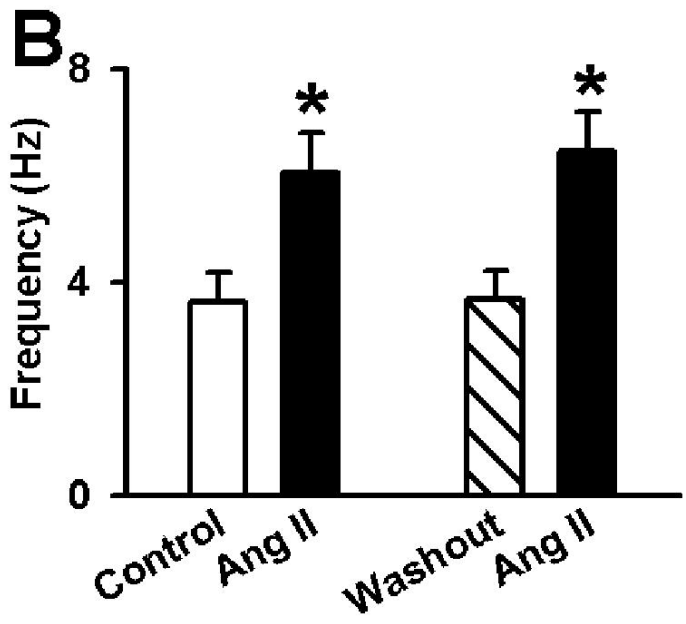

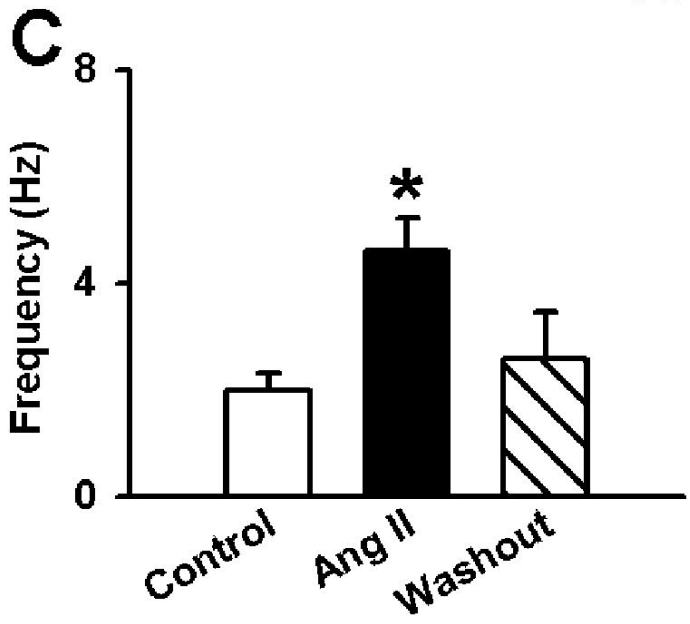

Fig. 2

JPET Fast Forward. Published on January 28, 2005 as DOI: 10.1124/jpet.104.082495
This article has not been copyedited and formatted. The final version may differ from this version.

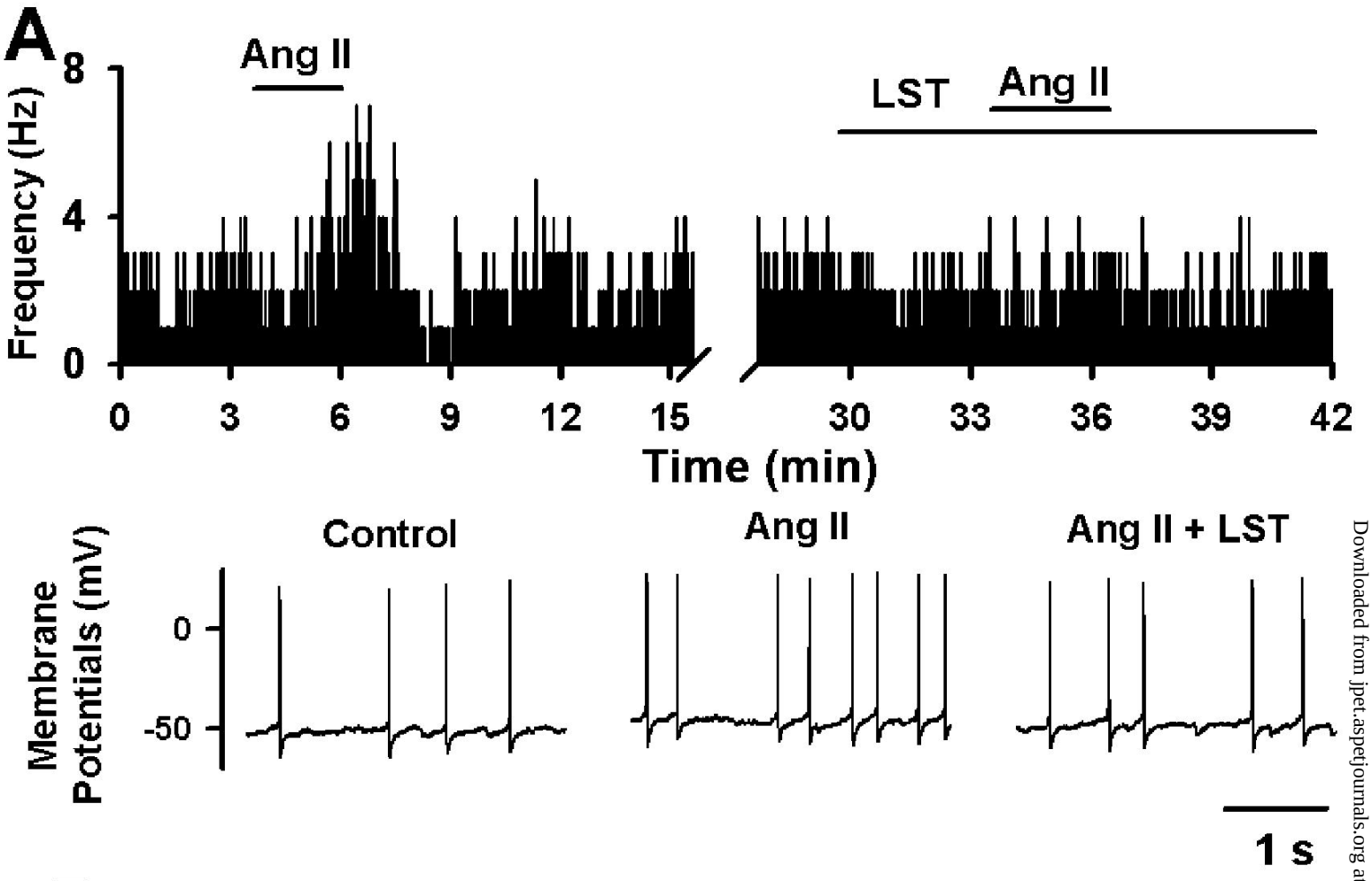

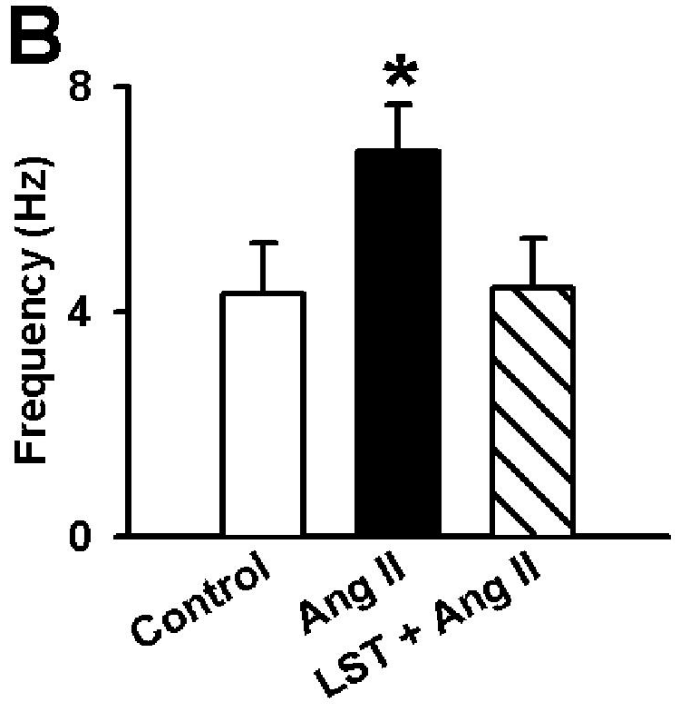

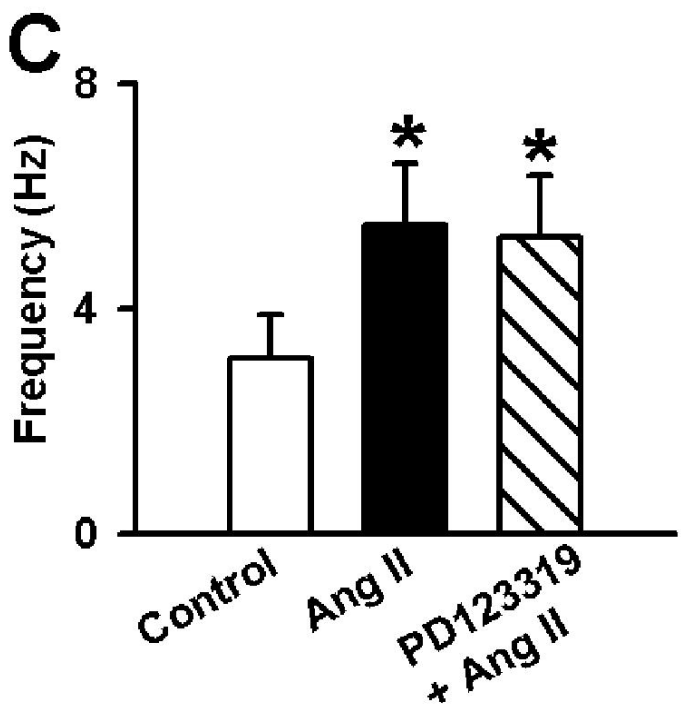

Fig. 3

JPET Fast Forward. Published on January 28, 2005 as DOI: 10.1124/jpet.104.082495
This article has not been copyedited and formatted. The final version may differ from this version.

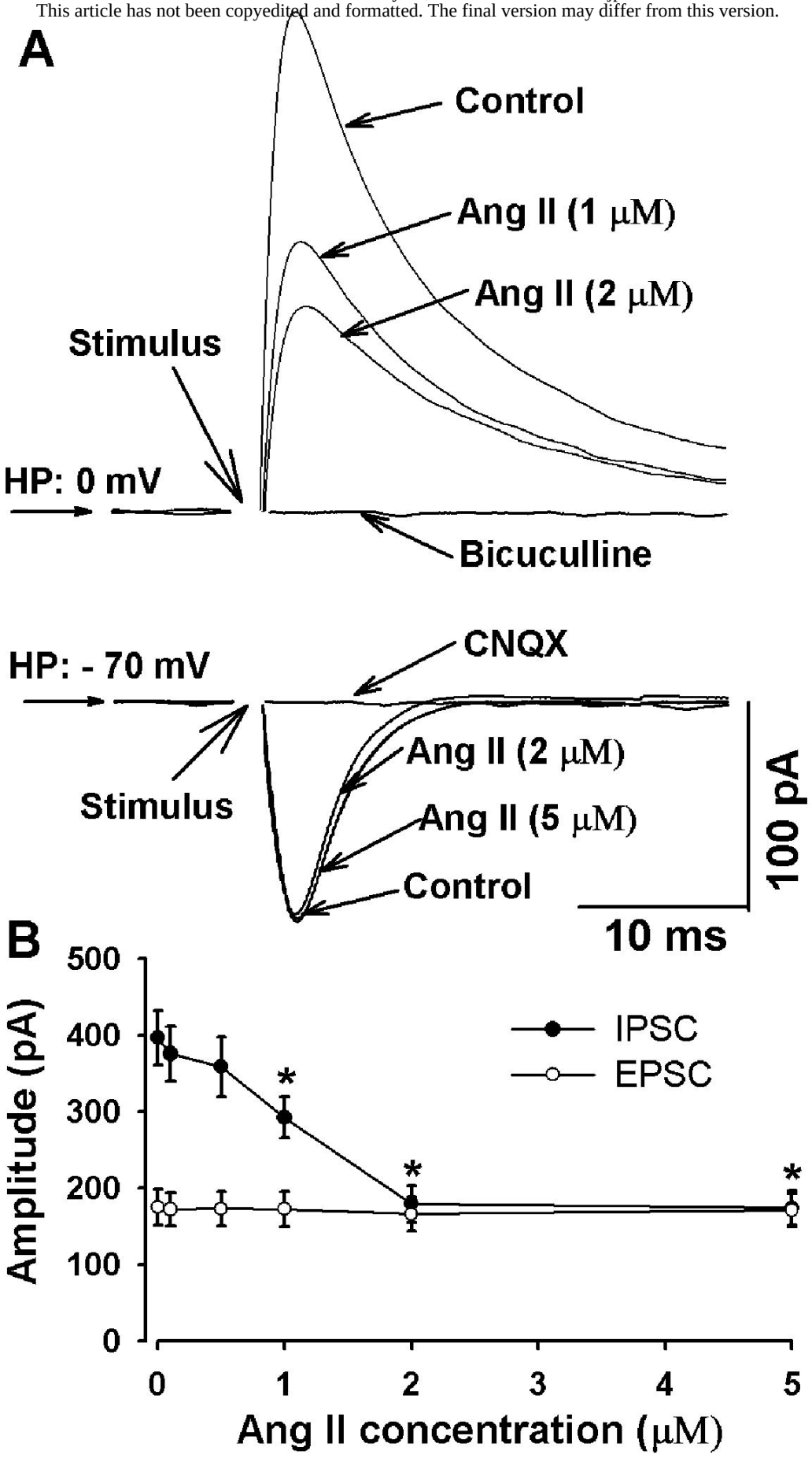

Fig. 4

JPET Fast Forward. Published on January 28, 2005 as DOI: 10.1124/jpet.104.082495
This article has not been copyedited and formatted. The final version may differ from this version.

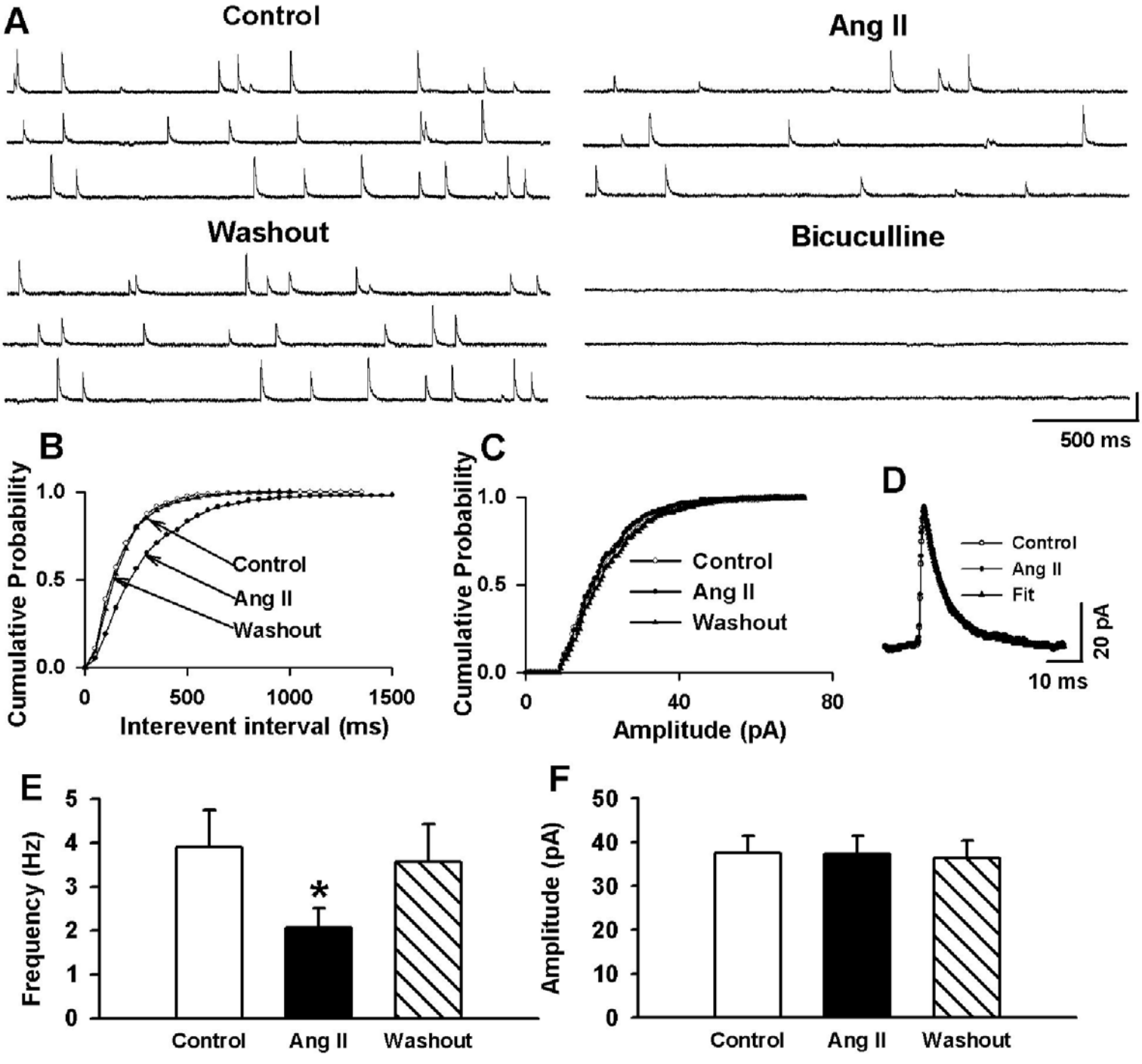

Fig. 5

JPET Fast Forward. Published on January 28, 2005 as DOI: 10.1124/jpet.104.082495
This article has not been copyedited and formatted. The final version may differ from this version.

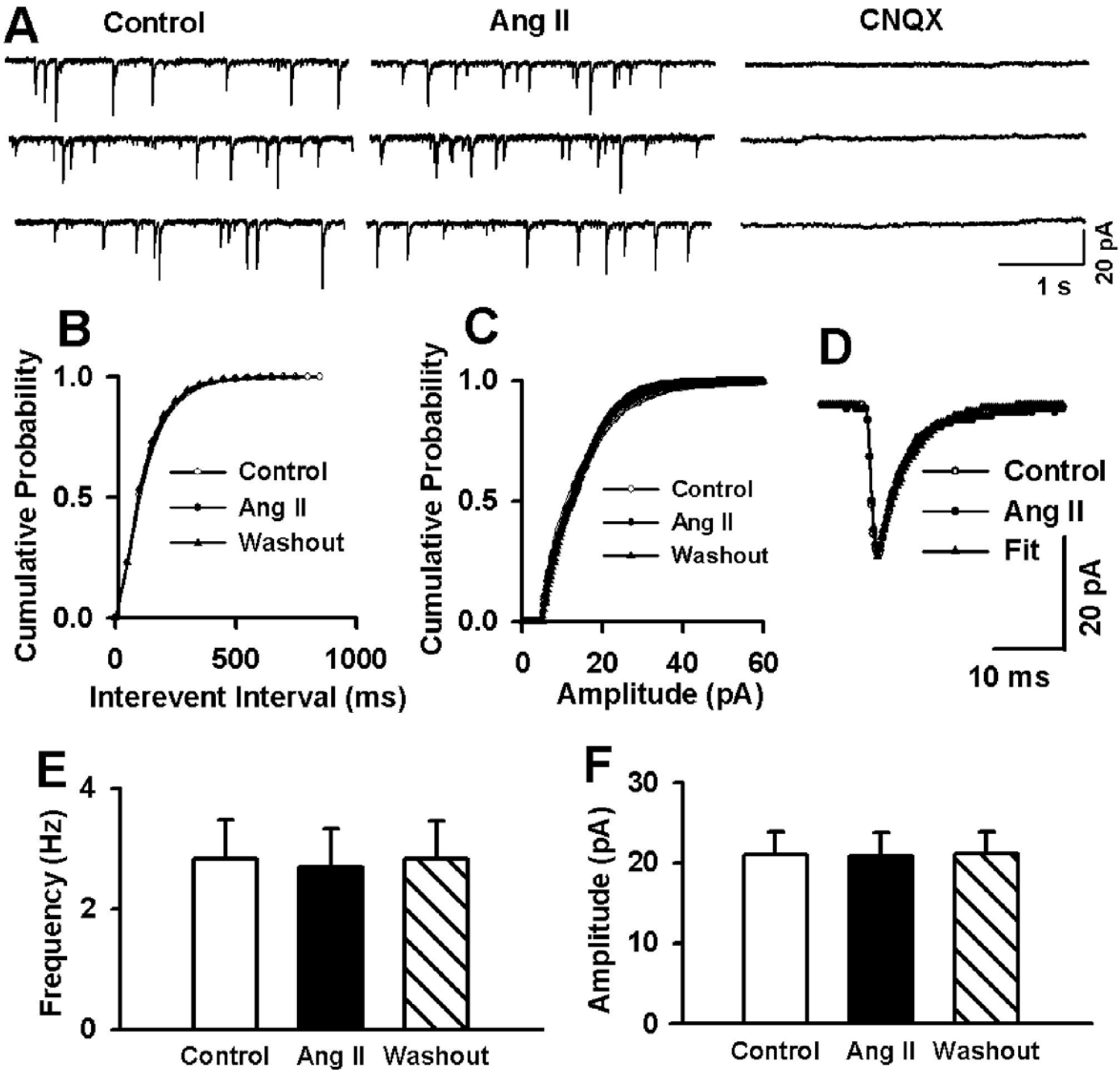

Fig. 6

JPET Fast Forward. Published on January 28, 2005 as DOI: 10.1124/jpet.104.082495
This article has not been copyedited and formatted. The final version may differ from this version.

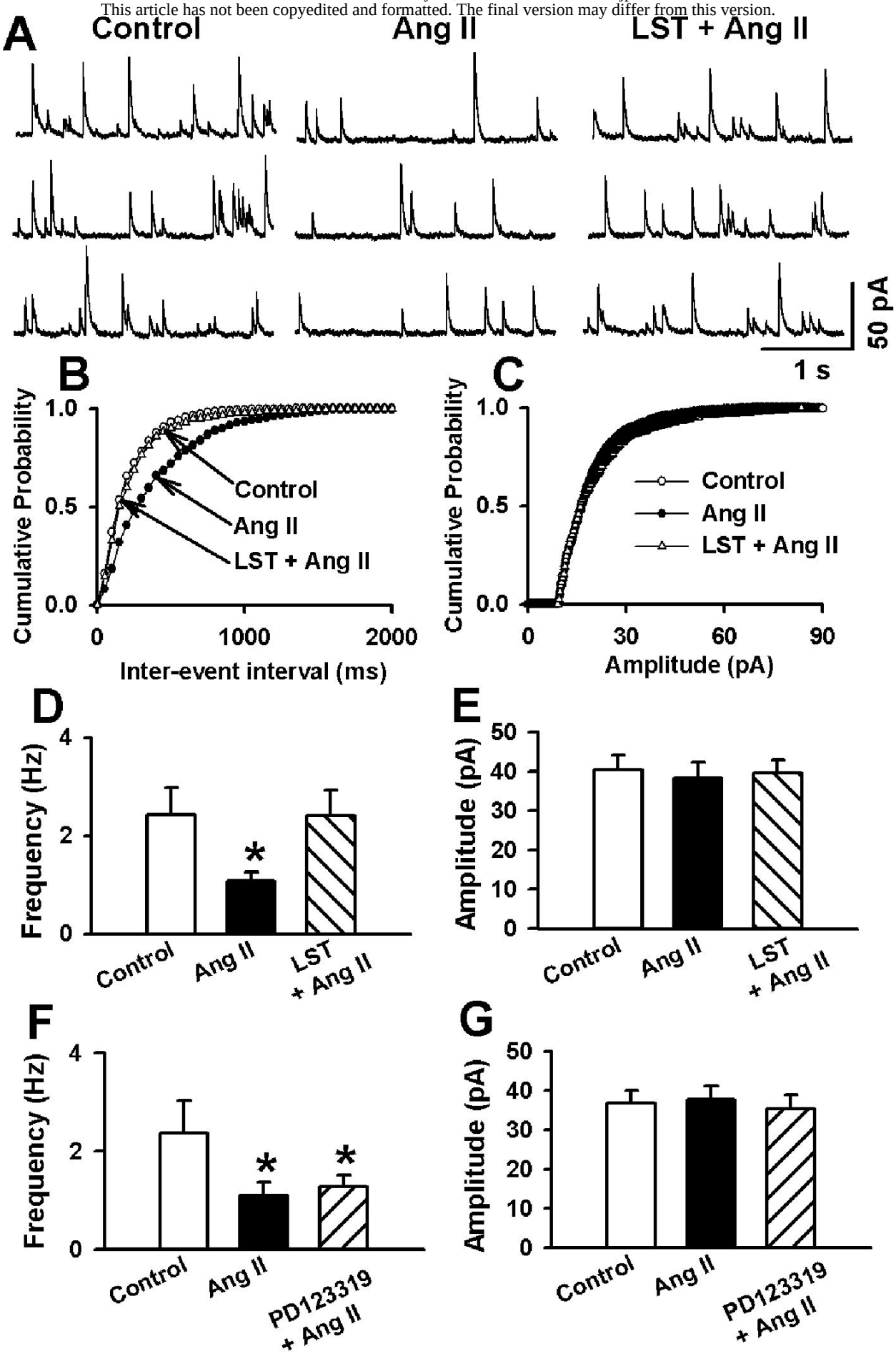

Fig. 7

JPET Fast Forward. Published on January 28, 2005 as DOI: 10.1124/jpet.104.082495
This article has not been copyedited and formatted. The final version may differ from this version.

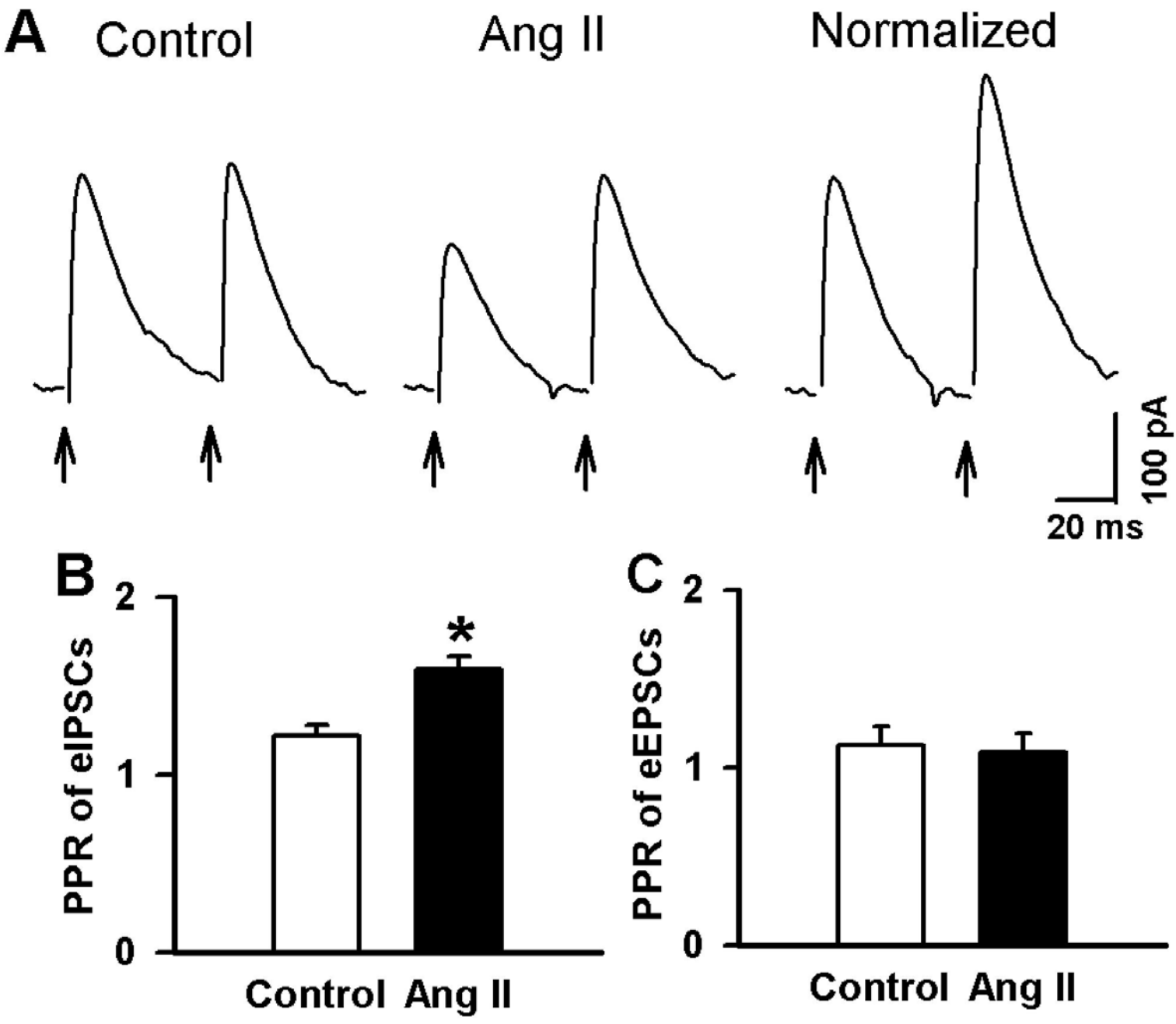

Fig. 8

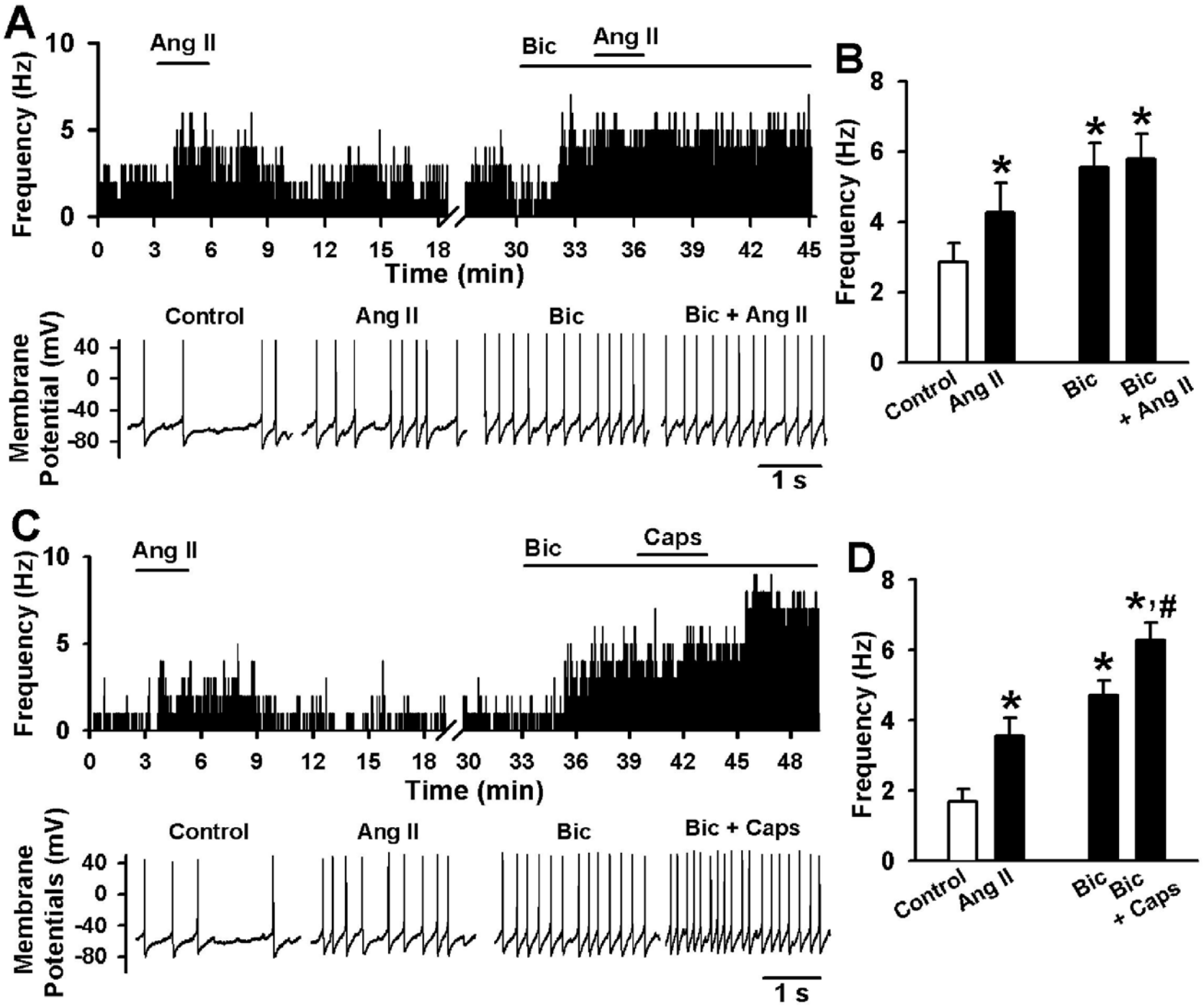

Fig. 9